Journal of Materials Chemistry A

Accepted Manuscript

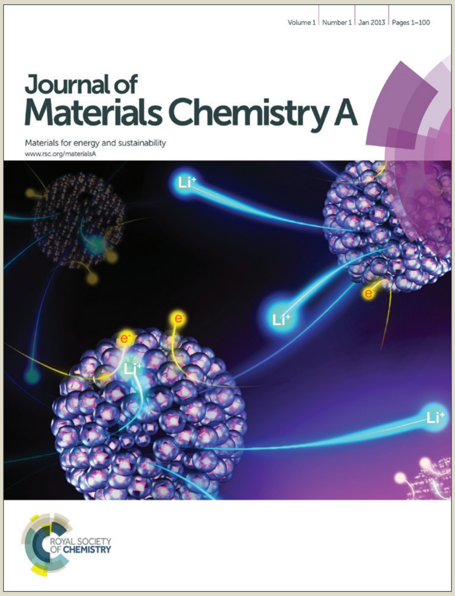

ROYAL SOCIETY OF CHEMISTRY

www.rsc.org/materialsA

Journal Name

RSCPublishing

ARTICLE

Cite this: DOI: 10.1039/x0xx00000x

Received 00th January 2012,
Accepted 00th January 2012

DOI: 10.1039/x0xx00000x

www.rsc.org/

In-situ assembly of monodispersed Ag nanoparticles in the channels of ordered mesopolymers as highly active and reusable hydrogenation catalyst

Xianchun Liu,[a,b] Renxi Jin,[b] Dashu Chen,[b] Lin Chen,[b] Shuangxi Xing,[b] Hongzhu Xing,[b] Yan Xing[b] and Zhongmin Su*[a,b]

In this study, we report a simple *in-situ* auto-reduction strategy for the fabrication of Ag@FDU-15 nanocomposites, in which the small sized Ag nanoparticles are monodispersed in the channels of FDU-15 ordered mesopolymer. The as-prepared Ag@FDU-15 nanocomposites were characterized by small and wide angle X-ray diffraction (XRD), nitrogen sorption, thermal gravimetric analysis (TGA), energy dispersive X-ray spectroscopy (EDS), X-ray photoelectron spectroscopy (XPS), transmission electron microscopy (TEM) and scanning transmission electron microscopy (STEM). TEM results show that the silver nanoparticles are uniformly dispersed with a mean diameter of 5.6 ± 0.5 nm. When used as hydrogenation catalyst, the Ag@FDU-15 nanocomposites exhibit excellent catalytic performance and reusability for the reduction of 4-nitrophenol (4-NP) in the presence of $NaBH_4$.

1. Introduction

Silver nanoparticles (Ag NPs) are considered as one of the most promising functional materials in electronic, chemical, biological and catalytic fields.[1-3] With the development of nanoscience and technology, nanoscaled silver particles have attracted extensive attention in the past decades due to their distinctive properties compared with the bulk phase. In the field of catalysis, Ag NPs have demonstrated great improvements in their catalytic performance for several chemical reactions, such as oxidative conversion of methanol into formaldehyde, partial oxidation of benzyl alcohols and oxidation of carbon monoxide.[4-6] However, two major difficulties are associated with the utilization of Ag NPs in catalysis. On the one hand, due to their high surface energy, Ag NPs tend to grow and form hard agglomerates, thus resulting in reducing their surface area and accessible active sites available for catalytic reactions;[7,8] On the other hand, it is difficult for small sized Ag NPs to be recovered from the reaction media, so their recycling is not suitable for large scale applications.[9] To solve these problems, a conventional way is to disperse Ag NPs on an appropriate support (such as silica gel, polymers, metal oxides, carbon, *etc.*)[10-15] to form composite catalysts, which seems to be the best method to avoid the aggregation of Ag NPs. Unfortunately, as these traditional supports are generally nonuniform in structure, the size of the obtained Ag NPs in most cases is randomly distributed, which not only reduces the metal atom efficiency but also may lead to undesired side reactions.[16] Hence, controlled synthesis of Ag NPs with small size and uniform dispersion is still a great challenge in catalyst design.

Recently, ordered mesoporous materials (OMMs) have attracted much attention because of their excellent physicochemical properties, such as large specific surface area, tuneable pore structures, thermal stability, and unusual surface topology.[17-20] They have opened new possibilities to get small sized Ag NPs with uniform dispersion. Generally, it is expected that Ag NPs can be confined in the channels of OMMs to prevent their aggregation and make the separation of the Ag NPs from the products more easily. To date, several OMMs have been used as support to immobilize the Ag NPs.[21-28] For example, Sun and co-workers directly used ordered mesoporous silica with inbuilt functionalities to anchor Ag NPs, where the small Ag NPs were loaded in the mesoporous and their aggregation was effectively prevented at high temperature.[21] Deng et al. prepared highly dispersed Ag supported nanocomposites by using functionalized ordered mesoporous carbon as support. The obtained Ag@ordered mesoporous carbon materials exhibited excellent stability and no metal leaching was detected even in harsher conditions.[22] To generate well dispersed Ag NPs into the channels of OMMs, the wet-chemistry approach has been commonly used where the silver precursors are impregnated in the OMMs and reduced by chemical treatments. However, some disadvantages exist in this process: the OMMs need premodification with functional groups (such as amino, carboxyl and so on) to anchor Ag NPs which is complicated in practical applications; furthermore, reduction of the silver ions into Ag NPs usually uses sodium borohydride, sodium citrate and formaldehyde as reducing agents, which may be associated with environmental toxicity or biological hazards. Therefore, it is highly desired to develop ways to minimize these problems. More recently, Meng and co-workers synthesized a novel ordered mesopolymer (FDU-15, Fudan University) by using cheap, soluble phenolic resins as precursor and commercially available triblock copolymer as a structure-directing agent through an evaporation induced self-assembly (ESIA) approach.[29] As a new class of ultra-stable mesoporous material, FDU-15 mesopolymer with plenty of surface functional groups offers a potential to serve as an alternative solid support for Ag NPs immobilization.[30] Herein, for the first time we report a simple *in-situ* auto-reduction strategy for the fabrication of monodispersed Ag NPs in the channels of FDU-15 ordered mesopolymer. The as-prepared Ag@FDU-15 nanocomposites exhibit excellent activity and reusability in catalyzing the reduction of 4-NP.

2. Experimental section

2.1 Chemicals

Poly(ethylene oxide)-b-poly(propylene oxide)-b-poly(ethylene oxide) triblock copolymers Pluronic F127 ($PEO_{106}PPO_{70}PEO_{106}$, Mw = 12600) was purchased from Sigma-Aldrich Co. Silver nitrate ($AgNO_3$, 99.8 wt %), phenol (C_6H_5OH, 99.98 wt %) and formalin solution (HCHO, 37 wt %) were purchased from Aladdin Industrial Corporation. Sodium hydroxide (NaOH, minimum 96 wt %), hydrochloric acid (HCl, 36–38 wt %), ammonia ($NH_3{\bullet}H_2O$, 25 wt %) and ethanol (C_2H_5OH, minimum 99.7 wt %) were purchased from Beijing Chemical Corporation. All chemicals were used as received without any further purification. Water used in all synthesis was distilled and deionised.

2.2 Resol precursor preparation

A soluble low-molecular-weight polymer (resol, Mw = 500-5000) derived from phenol and formaldehyde was prepared according to a reported method with minor revision.[28] Typical preparation procedure: Phenol (1 g) was melted at 48 °C before 20 wt % NaOH (aq, 0.21 g) was added slowly over 10 min with stirring. Formalin (37 wt %, 1.7 g) was added dropwise, and the reaction mixture was stirred at 78 °C for 1 h. After cooling the mixture to room temperature, the pH of the reaction mixture was adjusted to neutral (7.0) using 0.1 M HNO_3. Water was then removed under vaccum below 50 °C. The final product was redissolved in ethanol before use.

2.3 Synthesis of FDU-15 mesopolymer

FDU-15 mesopolymer was synthesized according to reference.[28] In a typical synthesis, 1.0 g of triblock copolymer F127 was dissolved in 20.0 g ethanol, and then 5.0 g of a 20 wt % resol ethanol solution was added with stirring for 10 min. The solution was transferred into a dish to evaporate the ethanol at room temperature for 5-8 h, and at further heating in an oven at 100 °C for 24 h. The products were collected and calcined 350 °C for 2 h at a heating rate of 1 °C min^{-1} in N_2.

2.4 Synthesis of Ag@FDU-15 nanocomposites

Ag@FDU-15 nanocomposites were prepared by an *in-situ* auto-reduction method. Typically, $Ag(NH_3)_2NO_3$ (aq, 10 μL) was added into a mixture of ethanol and water (1 mL, 1:1, v:v), then FDU-15 mesopolymer (2 mg) was added under stirring at 40 °C. After stirring for 10 min, the Ag@FDU-15 nanocomposites were obtained and rinsed with large amounts of deionised water and dried at 50 °C. $Ag(NH_3)_2NO_3$ (aq) solution was prepared by dropwise addition of NH_3 (aq) into $AgNO_3$ (aq, 2 wt %) solution until the formation of a clear colourless solution. In the control experiments, the same procedure was followed except that $AgNO_3$ (aq, 2 wt %) was used as silver source.

2.5 Catalytic property of Ag@FDU-15 nanocomposites

The catalytic reactions were conducted by mixing 4-NP aqueous solution (2 mL, 0.12 mM) with freshly prepared $NaBH_4$ aqueous solution (1 mL, 0.053 M) in a quartz cuvette. Subsequently, Ag@FDU-15 nanocomposites aqueous suspension (50 μL, 0.25 mg mL^{-1}) were injected to the above reaction mixture to start the reduction. The reduction in the optical absorption peak of 4-NP was determined from the UV-Vis spectrum using a UV-Vis spectrophotometer. Recycle catalysis experiments were conducted to study the reusability of the catalysts. The catalyst was separated by centrifugation after monitoring the whole reduction process and washed with water and ethanol several times, followed by drying overnight at 40 °C in vacuum oven. Finally, the catalyst was redispersed in a new reaction system for subsequent catalytic experiments under the same reaction conditions. The same procedures were repeated five times.

2.6 Characterization

X-ray powder diffraction (XRD) analysis was measured on a Siemens D5005 Diffractometer with Cu Kα radiation (λ = 1.5418Å). Transmission electron microscopic (TEM) images, high-resolution transmission electron microscopy (HRTEM) images and scanning transmission electron microscopy (STEM) images were obtained on a JEM-2100F microscope with an accelerating voltage of 200 kV. Energy dispersive X-ray spectroscopy (EDS) was conducted with Inca X-sight instrument made by Oxford Instruments. The nitrogen adsorption and desorption isotherms were measured at 77 K on a Micromeritics Tristar 3000 analyzer. The Brunauer–Emmett–Teller (BET) specific surface area was calculated using adsorption data. The pore size distribution curve was calculated from the analysis of the adsorption branch of the isotherm using the Barrett–Joyner–Halenda algorithm. A Thermo ESCALAB 250 X-ray photoelectron spectroscope (XPS) equipped with a standard and monochromatic source (Al Kα hν = 1486.6 eV) was employed for surface analysis. Thermao-gravimetric analysis (TGA) was carried out on a NETZSCH STA 449C thermoanalyzer in air. UV-Vis absorption spectra were measured at room temperature with a UV–Vis–NIR (Purkinje General, TU-1900) spectrophotometer.

3. Results and discussion

3.1 Preparation and characterization of Ag@FDU-15 nanocomposites.

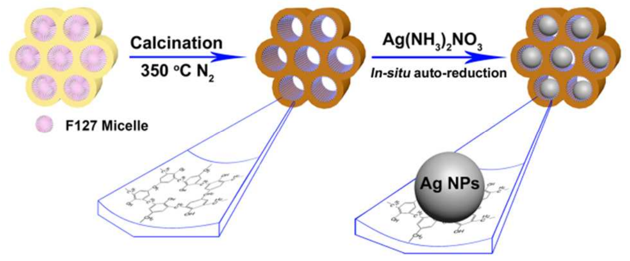

Scheme 1. Fabrication of the Ag NPs in the channels of FDU-15 mesopolymer.

The Ag@FDU-15 nanocomposites were prepared by impregnating FDU-15 mesopolymers with the aqueous solution of $Ag(NH_3)_2NO_3$, as shown in Scheme 1. There is no additional reducing agent needed during the process, the phenolic groups and the π-electrons of benzene ring in FDU-15 may act as reducing agent and stabilizer.[31,32] When reacting with these groups, $Ag(NH_3)_2NO_3$ was *in-situ* converted to the Ag NPs in the channels of FDU-15.

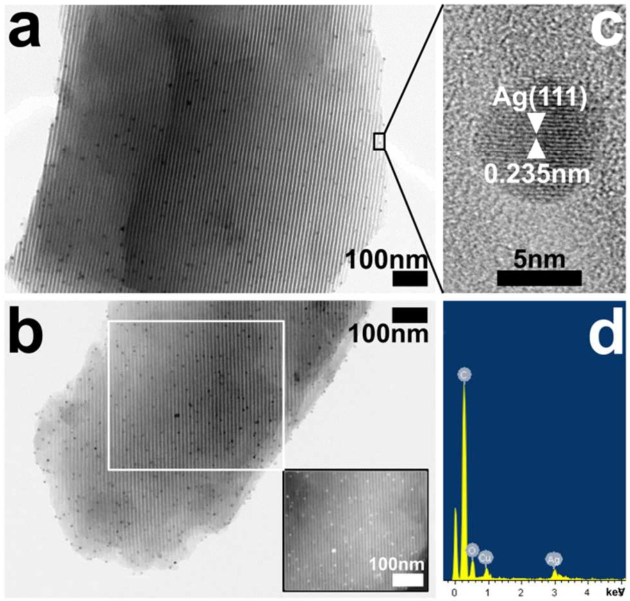

Fig. 1 TEM images (a, b), HRTEM image (c) and EDS pattern (d) of Ag@FDU-15 nanocomposites. Inset (b) is the HAADF-STEM image.

The morphology and distribution of the supported Ag NPs in FDU-15 were investigated using transmission electron microscopy (TEM) and scanning transmission electron microscopy (STEM). As shown in Fig. 1a and 1b, the small Ag NPs (dark spots) are monodispersed in the channels of FDU-15 and no visible aggregation is detected, which can be attributed to the “confinement effect” of the ordered mesoporous structure to prevent the growth of Ag NPs.[21] The diameter of Ag NPs is approximately 5.6 ± 0.5 nm according to the TEM image (see Fig. S1 in the supporting information). The high angle annular dark field STEM (HAADF-STEM) image (inset Fig. 1b) further confirms that the Ag NPs (bright spots) are uniformly distributed and anchored in the channels of the support. The high-resolution TEM (HRTEM) image (Fig. 1c) shows a representative particle of the square area in Fig. 1a, revealing the characteristic lattice fringes of 0.235 nm of Ag (111).[6] The energy-dispersive X-ray spectrum (EDS) (Fig. 1d) from the corresponding TEM image confirms that the Ag@FDU-15 nanocomposites are composed of C, O and Ag elements. The Cu peak comes from the copper grid.

In addition, we found that the silver source in our experiment plays a vital role in the controlling fabrication of mondispersed Ag NPs in the channels of FDU-15. Parallel experiment was carried out by substituting $Ag(NH_3)_2NO_3$ with $AgNO_3$. As shown in Fig. S2, several large Ag NPs were observed on the external surface of FDU-15. The main reason for this observation is likely that the reaction rate of Ag^+ and FDU-15 is too fast under these conditions. When $Ag(NH_3)_2NO_3$ was used, the coordination between the Ag^+ and NH_3 could decrease the release rate of Ag^+, thus, the Ag nuclei could undergo a relatively uniform growth stage, and finally, the Ag NPs with uniform size distribution could be obtained.[33]

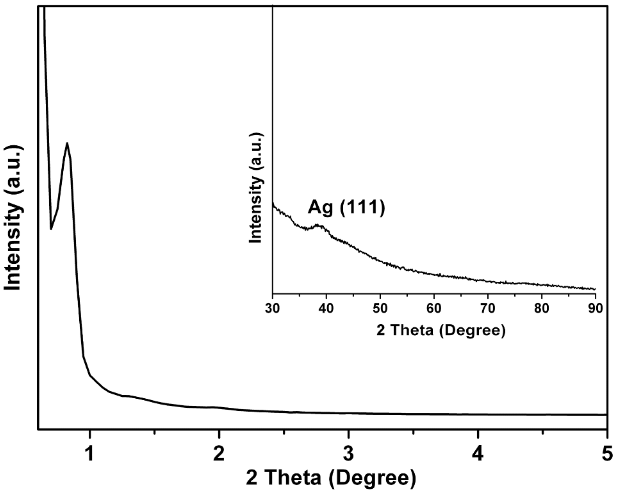

Fig. 2 SXRD pattern and WXRD pattern (inset) of Ag@FDU-15 nanocomposites.

The structure information of Ag@FDU-15 nanocomposites was collected using small-angle (SAXRD) and wide-angle XRD (WAXRD). The SAXRD pattern (Fig. 2) exhibits a typical low-angle reflection characteristic of 2D hexagonal symmetry in space group *P*6mm, indicating that the ordered mesostructure of FDU-15 was still maintained even after loaded with Ag NPs. The WAXRD pattern (inset Fig. 2) shows one diffraction peak at $2\theta = 38.3°$, which can be indexed as Ag (111) reflection.[6] The broad and weak XRD peaks may indicate that the supported Ag NPs have small particle size, which is in accordance with the TEM observations (Fig. 1a and b).

The X-ray photoelectron spectroscopy (XPS) measurement was used to further examine the chemical states of the silver species in the Ag@FDU-15 nanocomposites. Fig. 3 shows the XPS data of the Ag $3d_{5/2}$ and Ag $3d_{3/2}$ binding-energy regions. The binding energies of Ag $3d_{5/2}$ and Ag $3d_{3/2}$ are determined to be 368.4 and 374.5 eV, respectively. The spin energy separation is 6.1 eV, indicating that the formation of the metallic Ag NPs (Ag^0) in the channels of FDU-15.[15] In addition, the two peaks exhibit slight shift relative to the bulk silver (368.2 eV for $3d_{5/2}$ and 374.3 eV for $3d_{3/2}$), these may be partly from the interaction between the Ag NPs and FDU-15 support.[34]

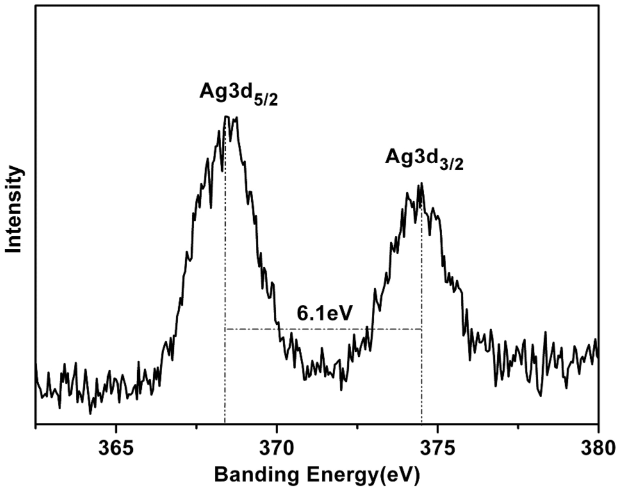

Fig. 3 Ag 3d XPS data of the Ag@FDU-15 nanocomposites.

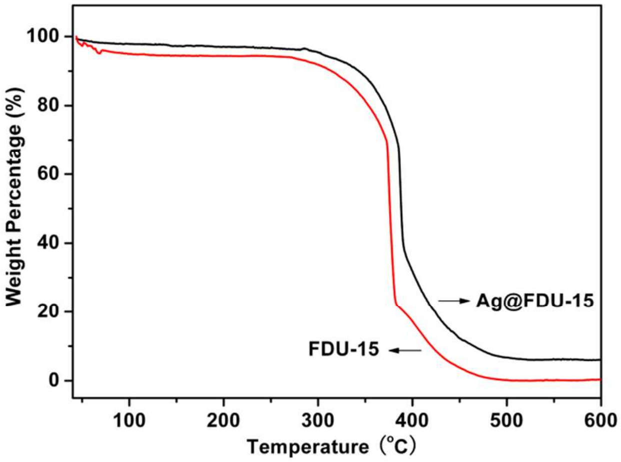

Fig. 4 TGA of the pure FDU-15 mesopolymer and Ag@FDU-15 nanocomposites.

The amount of Ag loaded in FDU-15 was measured by using thermo-gravimetric analysis (TGA). Fig. 4 shows the thermal behaviour of the pure FDU-15 mesopolymer and Ag@FDU-15 nanocomposites in air. A dramatic weight loss observed both in pure FDU-15 and Ag@FDU-15 nanocomposites in the temperature range of 350-500 °C is attributed to the decomposition of the polymer framework. There is no change in weight loss after 500 °C indicating the polymer framework has been completely decomposed. Compared with the pure FDU-15 mesopolymer, the remaining of Ag@FDU-15 with the content of 6 wt % should be pure silver.[35,36]

Fig. 5 shows the N_2 adsorption–desorption isotherms and pore size distributions of the pure FDU-15 mesopolymer and Ag@FDU-15 nanocomposites. Their corresponding pore structure parameters are summarized in Table 1. The Ag@FDU-15 nanocomposites display type-IV curve with distinct capillary condensation step in the relative pressure range of 0.6-0.8 and H1-type hysteresis loop, characteristic of mesoporous solids with uniform pore size.[29] This indicates that the ordered mesoporous structure has been maintained after the loading of Ag NPs. The adsorption and desorption isotherms of Ag@FDU-15 are not closed at the low relative pressures, which is attributed to the sample's polymer framework.[29,37] The pore diameter is calculated to be 6.4 nm with a narrow distribution, which further confirms that Ag NPs have been successfully confined in the mesoporous. The Brunauer-Emmett-Teller (BET) surface area and the pore volume of the Ag@FDU-15 nanocomposites are 413 m^2g^{-1} and 0.39 cm^3g^{-1}, respectively. Compared with the pure FDU-15 mesopolymer, there is only slight decrease in the surface area and pore volume. This suggests that the channels of the as-prepared Ag@FDU-15 nanocomposites remain open, which is important to allow the reactants diffusing into the support to reach the Ag NPs in the catalytic process.

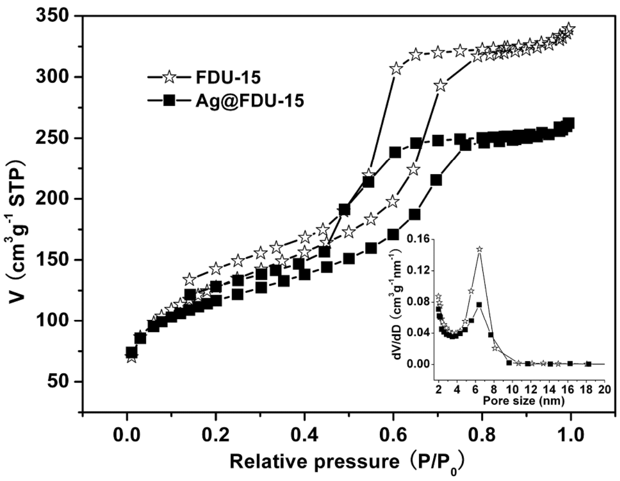

Fig. 5 Nitrogen sorption isotherms and pore size distribution curves (inset) of the pure FDU-15 mesopolymer and Ag@FDU-15 nanocomposites.

Table 1 Pore structure parameters of the pure FDU-15 mesopolymer and Ag@FDU-15 nanocomposites. (S_{BET}: BET surface area, V: pore volume, D_P: pore diameter)

Sample	S_{BET} (cm^2g^{-1})	V (cm^3g^{-1})	D_P (nm)
FDU-15	462	0.51	6.4
Ag@FDU-15	413	0.39	6.4

3.2 Application of Ag@FDU-15 nanocomposites for the catalytic reduction of 4-nitrophenol

It is well-known that 4-aminophenol (4-AP) has potential applications in medicine, corrosion inhibitors, and photographic developers.[38–40] Recently, Ag catalyst has been accepted as an alternative and eco-friendly route to produce 4-AP in industry.[15] Here, we chose the reduction of 4-NP to 4-AP by $NaBH_4$ in an aqueous solution as a model system to quantitatively evaluate the catalytic activity and stability of the Ag@FDU-15 nanocomposites. As shown in Fig. S3, the solution of 4-NP exhibits a strong absorption peak at 317 nm. Upon addition of excess amount of $NaBH_4$, the absorption peak shifts to 400 nm due to the formation of 4-nitrophenolate ions.[41] In the absence of catalysts, no changes in the 4-NP solution are observed even after two days. When a trace amount of the Ag@FDU-15 nanocomposites was added into the solution, the absorption at 400 nm decreases immediately with a concomitant increase in the peak of 4-AP at 295 nm with time. After 280 s, the peak corresponding to the nitro compound disappeared, indicating that the catalytic reduction of 4-NP has proceeded completely (Fig. 6a). Considering excess $NaBH_4$ was used ($C_{NaBH4}/C_{4\text{-}NP}$ = 220), pseudo-first-order kinetics could be applied for the evaluation of rate constants.[42] Fig. 6b shows the $\ln(C/C_0)$ and C/C_0 versus reaction time data for the reduction of 4-NP over Ag@FDU-15 nanocomposites. A linear correlation is found between $\ln(C/C_0)$ and reaction time, and the corresponding rate constant k is calculated to be 13.08×10^{-3} s^{-1}.

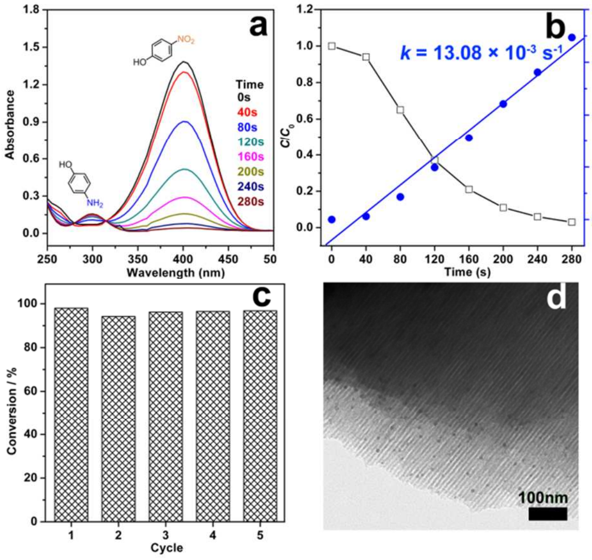

Fig. 6 UV-Vis absorption spectra during the catalytic reduction of 4-NP over Ag@FDU-15 (a); The $\ln(C/C_0)$ and C/C_0 versus reaction time for the reduction of 4-NP over Ag@FDU-15, respectively. C_0 and C are the absorption peak at 400 nm initially and at time t, respectively (b); The reusability of Ag@FDU-15 (c); TEM image of Ag@FDU-15 after five cycles of the catalytic reduction reactions (d)

The turnover frequency (TOF) of Ag@FDU-15 nanocomposites can reach 444 h^{-1}, which is higher than other substrate-supported Ag nanocatalysts reported in most previous studies (see Table 2). As shown in Table 2, we found that those Ag NPs with larger size and wider size distribution have lower catalytic activities; meanwhile, it is obvious that the Ag NPs supported on the hydrophilic supports possess higher catalytic activities than those on the hydrophobic supports. As we know, the reduction of 4-NP to 4-AP by $NaBH_4$ occurred on the surface of Ag NPs.[46] It suggested that the hydrophilic supports are benefit to the catalytic reaction than hydrophobic supports because they could absorb the reactants (Borohydride ions and 4-NP molecules) more easily on the surface of Ag NPs in the aqueous medium.[47] Therefore, we speculated that the excellent catalytic activity of Ag@FDU-15 nanocomposites may be attributed to the monodispersed and small sized Ag NPs, as well as the mesopore with relatively hydrophilic surface of FDU-15, which allows the effective contact between the reactants and Ag NPs in the reaction.

Table 2 Comparison of recent reports on Ag NPs catalyzed reduction 4-NP by $NaBH_4$.

Catalyst support	Size of Ag NPs (nm)	Support surface	k ($\times 10^{-3}$ s^{-1})	TOF (h^{-1})	Ref
Polymer nanocapsules	2-10	Hydrophilic	0.12	122.4	11
PZS nanotubes	5-20	Not defined	11.1	101.4	43
PVA	5	Hydrophilic	5.3	457	44
Iron Oxide	2-5	Not defined	2.38	12.9	12
Carbon sphere	10 ± 2	Hydrophobic	1.69	0.07	15
SNTs	3-25	Hydrophilic	16.2	104	45
CNFs	5-100	Hydrophobic	4.6	34.7	35
OMS	7	Hydrophilic	127.4	24.3	26
OMC	13.2	Hydrophobic	5.32	22	36
FDU-15	5.6 ± 0.5	Hydrophilic	13.08	444	This work

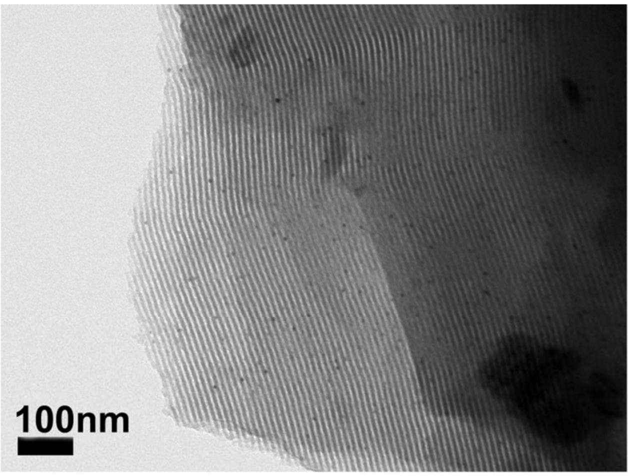

Fig. 7 TEM image of Ag@FDU-15 nanocomposites after heated at 500 °C for 2h in N_2

Furthermore, stability is also an important factor in the practical applications of catalysts. Here, we firstly investigated the cyclic stability of Ag@FDU-15 by using the nanocomposites five cycles. As shown in Fig. 6c, the catalytic activity of Ag@FDU-15 remains almost unchanged after running five cycles. The morphology of Ag@FDU-15 is retained and Ag NPs are still dispersed quite well in the channels of FDU-15, which is vital for high catalytic activity, even after being reused for five times (Fig. 6d). In addition, we also heated the as-prepared Ag@FDU-15 at 500 °C in N_2 for 2 h to investigate their thermostability. As shown in Fig. 7, the Ag NPs in the channels of FDU-15 maintain their dispersed state without obvious aggregation, which indicates that the Ag@FDU-15 have good thermal stability and resistance to sintering. The following factors may contribute to the excellent stability of the Ag@FDU-15: (1) The Ag NPs could be stabilized by the π-electrons of benzene ring and phenolic groups of FDU-15, which may lead to an enhanced stability against deactivation. (2) The "confinement effect" of mesoporous plays a key role in preventing the uncontrollable growth of the Ag NPs and improving their thermal stability.[21]

Conclusions

We have reported a simple *in-situ* auto-reduction strategy for the fabrication of Ag@FDU-15 nanocomposites, in which the small sized Ag NPs are monodispersed in the channels of FDU-15 mesopolymer. The results demonstrated that the phenolic groups and π-electrons of benzene ring in FDU-15 could be used as reduction agent and stabilizer to generate Ag NPs. The as-prepared Ag@FDU-15 nanocomposites exhibited excellent catalytic activity and reusability in the reduction of 4-NP. The success of Ag@FDU-15 nanocomposite represents a facile method for the preparation of monodispersed metal nanoparticles for catalytic applications.

Acknowledgements

This work was supported by the 863 Research Program of China (2013AA032204); The National Natural Science Foundation of China (Grant No. 21473027, 21473024, 21101023 and 21103018).

Notes and references

[a] College of Chemistry, Jilin University, Changchun, 130012, P. R. China; E-mail: zmsu@nenu.edu.cn.

[b] Department of Chemistry, Northeast Normal University, Changchun, 130024, P. R. China

Electronic Supplementary Information (ESI) available: Fig.S1-S3. See DOI: 10.1039/b000000x/

1 S. J. Yu, Y. G. Yin and J. F. Liu, *Environ. Sci.: Processes Impacts,* 2013, **15**, 78.
2 N. Yan, C. X. Xiao and Y. Kou, *Coord. Chem. Rev.,* 2010, **254**, 1179.
3 B. Wiley, Y. G. Sun and Y. N. Xia, *Acc. Chem. Res.,* 2007, **40**, 1067.
4 W. L. Dai, C. Yong, L. P. Ren, X. L. Yang, J. H. Xu, H. X. Li, H. Y. He and K. N. Fan, *J. Catal.,* 2004, **228**, 80.
5 R. Yamamoto, Y. Sawayama, H. Shibahara, Y. Ichihashi, S. Nishiyama and S. Tsuruya, *J. Catal.,* 2005, **234**, 308.
6 H. Y. Liu, D. Ma, R. A. Blackley, W. Z. Zhou and X. H. Bao, *Chem. Commun.,* 2008, **44**, 2677.
7 M. V. Canamares, J. V. Garcia-Ramos, J. D. Gomez-Varga, C. Domingo and S. Sanchez-Cortes, *Langmuir,* 2005, **21**, 8546.
8 P. L. Redmond, A. J. Hallock and L. E. Brus, *Nano Lett.,* 2005, **5**, 131.
9 A. C. Patel, S. X. Li, C. Wang, W. J. Zhang and Y. Wei, *Chem. Mater.,* 2007, **19**, 1231.
10 N. H. Khdary and M. A. Ghanem, *J. Mater. Chem.* 2012, **22**, 12032.
11 Y. Y. Gao, X. B. Ding, Z. H. Zheng, X. Cheng and Y. X. Peng, *Chem. Commun.*, 2007, **43**, 3720.
12 J. R. Chiou, B. H. Lai, K. C. Hsu and D. H. Chen, *J. Hazard. Mater.,* 2013, **248**, 394.
13 J. Y. Zhang, F. X. Xiao, G. C. Xiao and B. Liu, *Nanoscale,* 2014, **6**, 11293.
14 S. T. Zhang, R. W. Fu, D. C. Wu, W. Xu, Q. W. Ye and Z. L. Chen, *Carbon*, 2004, **42**, 3209.
15 S. C. Tang, S. Vongehr and X. K. Meng, *J. Phys. Chem. C,* 2010, **114**, 977.
16 X. F. Yang, A. Q. Wang, B. T. Qiao, J. Li, J. Y. Liu and T. Zhao, *Acc. Chem. Res.,* 2013, **46**, 1740.
17 U. Ciesla and F. Schuth, *Microporous Mesoporous Mater.,* 1999, **27**, 131.
18 A. Taguchi and F. Schuth, *Microporous Mesoporous Mater.,* 2005, **77**, 1.
19 J. M. Sun and X. H. Bao, *Chem. Eur. J.,* 2008, **14**, 7478.
20 C. Perego and R, Millini, *Chem. Soc. Rev.,* 2013, **42**, 3956.
21 J. M. Sun, D. Ma, H. Zhang, X. M. Liu, X. W. Han, X. H. Bao, G. Weinberg, N. Pfander and D. S. Su, *J. Am. Chem. Soc.,* 2006, **128**, 15756.
22 Y. H. Deng, Y. Cai, Z. K. Sun, D. Gu, J. Wei, W. Li, X. H. Guo, J. P. Yang and D. Y. Zhao, *Adv. Funct. Mater.,* 2010, **10**, 3658.
23 G. P. Yong, D. Tian, H. W Tong and S. M. Liu, *J. Mol. Catal. A: Chem.*, 2010, **323**, 40.
24 J. W. Zheng, H. Q. Lin, X. L. Zheng, X. P. Duan and Y. Z. Yuan, *Catal. Commun.,* 2013, **40**, 129.
25 A. Y. Yin, C. Wen, W. L. Dai and K. N. Fan, *Appl. Catal. B,* 2011, **108**, 90.
26 B. Naik, S. Hazra, V. S. Prasad and N. N. Ghosh, *Catal. Commun.,* 2011, **12**, 1104.
27 Y. Tian, J. J. Qi, W. Zhang, Q. Cai and X. Y. Jiang, *ACS Appl. Mater. Interfaces,* 2014, **6**, 12038.
28 J. R. Deka, H. M. Kao, S. Y. Huang, W. C. Chang, C. C. Ting, P. C. Rath and C. S. Chen, *Chem. Eur. J.,* 2014, **20**, 894.
29 Y. Meng, D. Gu, F. Q. Zhang, Y. F. Shi, H. F. Yang, Z. Li, C. Z. Yu, B. Tu and D. Y. Zhao, *Angew. Chem. Int. Ed.,* 2005, **44**, 7053.
30 I. Muylaert, A. Verberckmoes, J. D. Decker and P. V. D. Voort, *Adv. Colloid Interface Sci.,* 2012, **175**, 39.
31 Q. Dong, H. L. Su and D. Zhang, *J. Phys. Chem. B,* 2005, **109**, 17429.
32 R. Xing, Y. M. Liu, H. H. Wu, X. H. Li, M. Y. He and P. Wu, *Chem. Commun.,* 2008, **44**, 6297.
33 B. Chen, X. L. Jiao and D. R. Chen, *Cryst. Growth Des.,* 2010, **10**, 3378.
34 K. Y. Lee, M. Kim, J. Hahn, J. S. Suh, I. Lee, K. Kim and S. W. Han, *Langmuir,* 2006, **22**, 1817.
35 P. Zhang, C. L. Shao, Z. Y. Zhang, M. Y. Zhang, J. B. Mu, Z. C. Guo, Y. C. Liu, *Nanoscale* **2011**, *3*, 3357-3363.
36 Y. Chi, J. C. Tu, M. G. Wang, X. T. Li and Z. K. Zhao, *J. Colloid Interface Sci.,* 2014, **423**, 54.
37 Y. Meng, D. Gu, F. Q. Zhang, Y. H. Shi, L. Cheng, D. Feng, Z. X. Wu, Z. X. Chen, Y. Wan, A. Stein and D. Y. Zhao, *Chem. Mater.,* 2006, **18**, 4447.
38 Y. Du, H. L. Chen, R. Z. Chen and N. P. Xu, *Appl. Catal. A,* 2004, **277**, 259.
39 C. V. Rode, M. J. Vaidya and R. V. Chaudhari, *Org. Process Res. Dev.,* 1999, **3**, 465.
40 J. F. Corbett, *Dyes Pigments,* 1999, **41**, 127.
41 R. X. Jin, Y. Yang, Y. C. Zou, X. C. Liu and Y. Xing, *Chem. Eur. J.,* 2014, **20**, 2344.
42 J. P. Ge, Q. Zhang, T. R. Zhang and Y. D. Yin, *Angew. Chem. Int. Ed.,* 2008, **47**, 8924.
43 M. H. Wang, J. W. Fu, D. D. Huang, C. Zhang and Q. Xu, *Nanoscale,* 2013, **5**, 7913.
44 E. Hariprasad and T. P. Radhakrishnan, *Chem. Eur. J.,* 2010, **16**, 14378.

45 Z. Y. Zhang, C. L. Shao, Y. Y. Sun, J. B. Mu, M. Y. Zhang, P. Zhang, Z. C. Guo, P. P. Liang, C. H. Wang and Y. C. Liu, *J. Mater. Chem.,* 2012, **22**, 1387.

46 P. Hervés, M. Pérez-Lorenzo, L. M. Liz-Marzán, J. Dzubiella, Y. Lu and M. Ballauff, *Chem. Soc. Rev.,* 2012, **41**, 5577.

47 S. H. Zhang, S. L. Gai, F. He, S. J. Ding, L. Li and P. P. Yang, *Nanoscale*, 2014, **6**, 11181.

Graphical Abstract

In-situ assembly of monodispersed Ag nanoparticles in the channels of ordered mesopolymers as highly active and reusable hydrogenation catalyst

Xianchun Liu,[a, b] Renxi Jin,[b] Dashu Chen,[b] Lin Chen,[b] Shuangxi Xing,[b] Hongzhu Xing,[b] Yan Xing[b] and Zhongmin Su*[a, b]

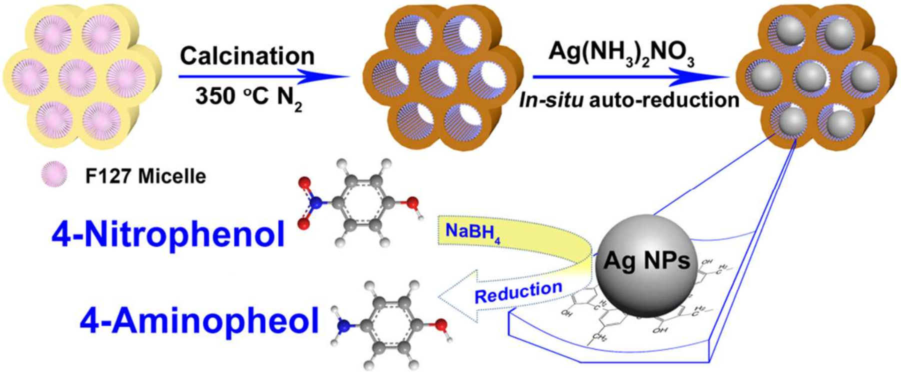

Monodispersed Ag nanoparticles were assembled in the channels of FDU-15 ordered mesopolymers by a simple *in-situ* auto-reduction method and exhibited high catalytic performance for the reduction of 4-nitrophenol.